AMSE JOURNALS-2016-Series: Modelling B; Vol. 85; N°1; pp 105-122
Submitted Oct. 2015; Revised Jan. 2, 2016, Accepted Nov. 15, 2016

Wire Coating Analysis in MHD Flow and Heat Transfer of a Third Grade Fluid with Variable Viscosity in a Porous Medium with Internal Heat Generation/Absorption and Joule Heating

M. K. Nayak

Department of Physics, Radhakrishna Institute of Technology and Engineering, Biju Patnaik University of Technology, Odisha, India.
E-mail: mkn2122@gmail.com

Abstract

In this paper, the wire coating analysis in MHD flow and heat transfer of a third grade fluid with variable viscosity in a porous medium with internal heat generation/absorption and Joule heating has been investigated. In the present study wire coating is carried out using melt polymer satisfying third grade fluid model. In the present discussion (i) Reynolds Model (ii) Vogel's Model are considered to account for temperature dependent viscosity. The boundary layer equations governing the flow and heat transfer phenomena are solved numerically by employing fourth order Runge-Kutta method and the effects of pertinent parameters such as permeability parameter, internal heat generation/absorption parameter and temperature dependent viscosity parameters on wire coating have been analyzed and are displayed with the help of graphs. It is important to remark that an increase in non-Newtonian parameter increases the velocity in the absence of porous matrix which agrees well with the results reported earlier but in the presence of porous matrix the velocity decreases in the entire span of the flow domain. One of the important aspects of the present study is that thermal boundary layer generates energy which causes an enhancement in temperature with an increase in heat generation parameter whereas for the case of heat absorption, the temperature falls. Further, the flow instability in the flows of extrusion die is well marked in case of Vogel's model as pointed out by Nhan-Phan-Thien.

Keywords: Wire coating, Third grade fluid, Porosity, Heat generation/absorption.

1. Introduction

Investigation on boundary-layer behaviour of a viscoelastic fluid over a continuously stretching surface finds many important applications in polymeric extrusion, drawing of plastic films and wires. The ever increasing applications in these industrial processes have led to renewed interest in the study of viscoelastic fluid flow and heat transfer in the wire coating process. Wire coating process is an industrial process to coat a wire for insulation, mechanical strength and environmental safety. Usually, three different processes are used for wire coating. They are such as

- Coaxial extrusion process
- Dipping process and
- Electro-statistical deposition process

The co-extrusion process operates at maximum possible pressure, temperatures and speeds. In this process of coating, the velocity of continuum and the melt polymer develop high pressure in a specific region which in turn produces strong bonding and imparts fast coating. The co-extrusion process studied by Han and Rao [1], Caswell and Tanner [2], Tucker [3], Nayak [4] is an operation in which either the polymer is extruded on axially moving wire or the wire is dragged inside a die

filled with molten polymer. The efficiency of coextrusion process can be enhanced by adopting hydrodynamic model by Akter and Hashmi [5]. The experimental set-up of a typical wire coating process is shown in Fig.1.

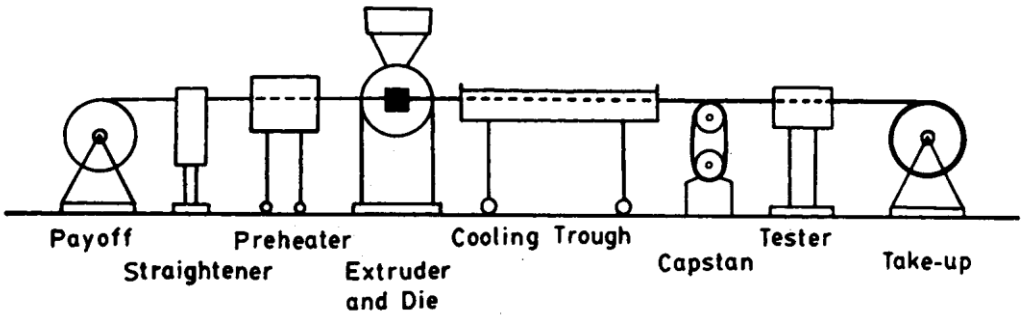

Fig. 1 Typical wire coating process.

In this set-up, the uncoated wire unwinds at the payoff reel passing through straightener, a preheater, a cross head die where it meets the melt polymer and emerges from the extruder and gets coated. This coated wire then passes through a cooling through, a capstan (puller) and a tester and is finally ends on the rotating take-up reel. The co-extrusion process is simple to apply, time saving and economical in view of industrial applications. Many researchers namely Tadmor and Gogos [6], Fata et al. [7], Siddiqui et al. [8] have therefore analyzed wire coating using third grade fluid.In wire coating, the quality of material and wire drawing velocity are important within the die. After leaving the die, the temperature of the coating material is also important.

Nomenclature

R_w	radius of the wire	ρ	density of the fluid
U_w	wire velocity	p	pressure
θ_w	wire temperature	F	viscous force per unit volume
L	length of die	k	thermal conductivity
R_d	radius of die	C_p	specific heat at constant pressure
θ_d	flow temperature	ϕ	dissipation function
B_0	strength of uniform transverse magnetic field	J	current density
		q	velocity of fluid
$\vec{B}$	magnetic field		
S	extra stress tensor	σ	electrical conductivity
θ	fluid temperature	β_0	non-Newtonian parameter/ perturbation parameter
K_p	permeable parameter		
μ	coefficient of Viscosity	M	magnetic parameter
μ	dynamic viscosity	Q	heat generation/absorption parameter

Third-grade fluid considered here represents a viscoelastic fluid of industrial importance. Many fluids used in wire-coating exhibit the characteristics of third grade fluid. Many authors [9]-[11] have studied in the field of third grade fluid. Recently, a visco-elastic fluid model known as Phan-Thien-Tanner (PTT) model is widely used for wire coating. It is a non-linear viscoelastic model which incorporates not only shear thinning, shear viscosity and normal stress difference but also an elongational parameter and so reproduces many of the characteristics of the rheology of

polymer solutions and other non-Newtonian fluids. Many authors have contributed to enrich the field of heat transfer of post-treatment analysis of wire coating. Kasajima and Ito [12] have worked on post-treatment of polymer extrudate in wire coating. They also performed a heat transfer analysis for the cooling of the coating. Wagner and Mitsoulis [13] have studied the effect of die design on the analysis of wire coating.

Bagley and Storey [14] provided numerical solutions for a Newtonian fluid in the form of dimensionless parameters characterizing the wire speed, die dimensions, radial position, shear rate, and melt viscosity. Tadmor and Bird [15] examined the effect of visco-elasticity on the eccentricity of the wire. Using the Criminale-Ericksen-Filbey (CEF) constitutive equation, they concluded that the lateral forces acting on the wire tend to stabilize it into a concentric position.

The properties of the final product are known to depend greatly on the rate of cooling in manufacturing processes. The central cooling system is beneficial to facilitate the process for a designed product. An electrically conducting polymeric liquid seems to be a good candidate for some industrial applications such as in polymer technology and extrusion processes because the flow can be regulated by external means through a magnetic field. The applied magnetic field may play an important role in controlling momentum and heat transfer in the boundary layer flow of different fluids in the process of wire coating. The study of flow and heat transfer in porous media has received much attention due to its enormous applications in diversified industries and contemporary technology. Porous materials can be used to enhance the heat transfer from the surface of the wire. In view of this, many authors have explored the effect of transverse magnetic field and porous matrix on Newtonian and non-Newtonian fluids. The effect of porosity was examined by several authors [16-20]. The effects of magnetic field, heat generation/absorption on flow and heat transfer of viscous electrically conducting fluids over several solid surfaces are examined by authors [21-24].

Nayak et al. [25] have considered third grade fluid as coating material in wire coating analysis and investigated there the MHD flow and heat transfer with temperature dependent viscosity. However, they have not investigated the effects of porous matrix and heat generation/absorption in their study. The objective of the present study is to analyze the wire coating process where a coating material modeled as third grade fluid such as melt polymer. The study is carried out considering constant viscosity and temperature dependent viscosity by using Reynolds and Vogel's models.

The novelty of the present study comprises the following aspects:

1. The porous matrix is included because it acts as an insulator due to which the flow and heat transport processes greatly prevents heat loss and accelerates the process of cooling/heating as the case may be serving as a heat exchanger. Also the permeability of a porous medium reduces the flow instability.
2. Heat generation/absorption is included because it controls the heat transfer rates in the thermal boundary layer appreciably.

The method of solution used here is fourth order Runge-Kutta method associated with shooting technique. The effects of non-Newtonian parameter, Reynolds model viscosity parameter, Vogel's model viscosity parameter, magnetic parameter, permeability parameter, heat generation/absorption parameter and Brinkman number on velocity and temperature distributions are presented.

2. Formulation of the Problem

The schematic diagram of the flow geometry is shown in Fig. 2. The wire of radius R_w is extruded along the central line with velocity U_w, temperature θ_w in a bath of third grade fluid such as molten polymer like polyvinyl chloride (PVC) in a porous medium inside a stationary pressure type die of finite length L having radius R_d and temperature θ_d. The fluid is acted upon by a constant pressure gradient $\frac{dp}{dz}$ in the axial direction and a transverse magnetic field of strength B_0. The magnetic field is perpendicular to the direction of incompressible flow. The magnetic Reynolds number is taken to be small enough so that the induced magnetic field can be neglected. Thus, in the present set up, the Lorentz force comes into play affecting the coating process.

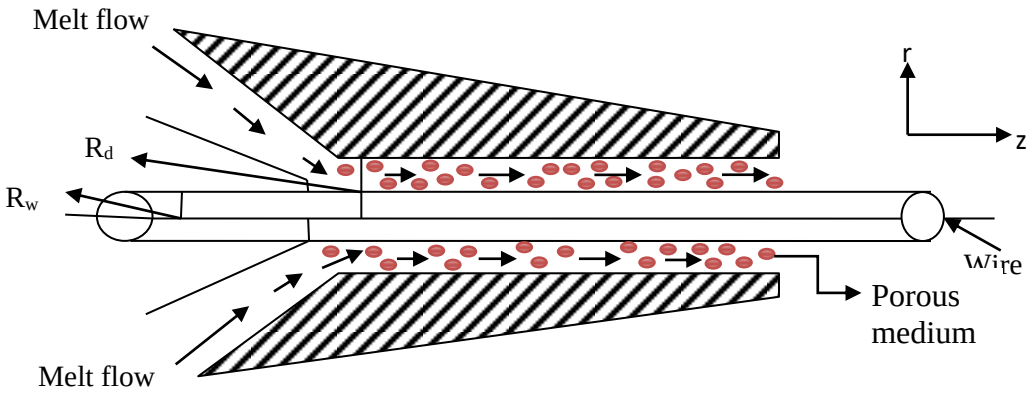

Fig. 2 Wire coating process in a porous medium in a pressure type die.

The die is filled with an incompressible third grade fluid. The wire and die are concentric and the co-ordinate system is chosen at the center of the wire in which r is taken perpendicular to the direction of the fluid flow and z-axis is along the flow. The flow is considered steady, laminar and axisymmetric.

The design of wire coating dies is of primary importance since it greatly affects the quality of the final product. The pressure type die is considered because within this die the melt meets the wire where a complex flow field exists and its surrounding is necessary for the design of better dies with optimum performance. Let us avoid excessive shear stresses at the wire which may lead to elongation or frequent breakage of the wire during coating operation and also excessive wall shear stress which may result in uneven and rough extrudate coating.

Assuming that no-slip boundary conditions are imposed on the moving wire and stationary die wall in the die region between the contact of the melt with the wire and die exit.

With the above mentioned frame of reference and assumptions the fluid velocity, extra stress tensor and temperature field are considered as

$$\vec{q} = [0,0,w(r)],\ S = S(r),\theta = \theta(r) \tag{1}$$

Boundary conditions are:

$$\left.\begin{aligned} w = U_w,\ \theta = \theta_w \ \ at\ \ r = R_w, \\ w = 0,\ \theta = \theta_d \ \ at\ r = R_d \end{aligned}\right\} \tag{2}$$

For third grade fluid, the extra stress tensor *S* is defined as

$$S = \mu A_1 + \alpha_1 A_2 + \alpha_2 A_1^2 + \beta_1 A_3 + \beta_2 \left(A_1 A_2 + A_2 A_1 \right) + \beta_3 \left(t_r A_2 \right) A_1 \tag{3}$$

in which $\alpha_1, \alpha_2, \beta_1, \beta_2, \beta_3$ are the material constants and A_1, A_2, A_3 are the kinematic tensors.

$$A_1 = L^T + L \tag{4}$$

$$A_n = A_{n-1} L^T + L A_{n-1} + \frac{D A_{n-1}}{Dt}, \; n = 2,3, \tag{5}$$

where the superscript *T* denotes the transpose of the matrix.

The basic equations governing the flow of an incompressible fluid are:

$$\vec{\nabla}.\vec{q} = 0 \tag{6}$$

$$\rho \frac{D\vec{q}}{Dt} = -\vec{\nabla} p + \vec{F} + \vec{J} \times \vec{B} + \frac{\mu \vec{q}}{K_p^*} \tag{7}$$

$$\rho C_p \frac{D\theta}{Dt} = k \, \nabla^2 \theta + \phi + Q_0 \left(\theta - \theta_w \right) + J_d \tag{8}$$

where $\vec{q}$ is the velocity vector, $\frac{D}{Dt}$ denotes substantial acceleration and Q_0 is the rate of volumetric heat generation/absorption and J_d is the Joulean dissipation term.

In the equation of motion (7) a body force $\vec{J} \times \vec{B}$ per unit volume of electromagnetic origin appears due to the interaction of the current and the magnetic field. The electrostatic force due to charge density is considered to be negligible. A uniform magnetic field of strength of B_0 is assumed to be applied in the positive radial direction normal to the wire i.e., along z-axis. Hence the retarding force per unit volume acting along z-axis is given by

$$\vec{J} \times \vec{B} = (0, 0, -\sigma B_0^2 w) \tag{9}$$

Using the velocity field (1), the continuity equation (6) is satisfied identically and the non zero components of extra tensor S from equation (3) are given by

$$S_{rr} = \left(2\alpha_1 + \alpha_2 \right) \left(\frac{dw}{dr} \right)^2 \tag{10}$$

$$S_{zz} = \alpha_2 \left(\frac{dw}{dr} \right)^2 \tag{11}$$

$$S_{rz} = \mu \frac{dw}{dr} + 2\left(\beta_2 + \beta_3 \right) \left(\frac{dw}{dr} \right)^3 \tag{12}$$

Substituting the velocity field and equations (9) – (12) in the equation of balance of momentum (7), we obtain

$$\frac{-\partial p}{\partial r} = \left(2\alpha_1 + \alpha_2 \right) \frac{1}{r} \frac{d}{dr} \left\{ r \left(\frac{dw}{dr} \right)^2 \right\} \tag{13}$$

$$\frac{\partial p}{\partial \theta} = 0 \tag{14}$$

$$\frac{\partial p}{\partial z} = \frac{1}{r} \frac{d}{dr} \left(r \mu \frac{dw}{dr} \right) + \frac{2\left(\beta_2 + \beta_3 \right)}{r} \frac{d}{dr} \left(r \left(\frac{dw}{dr} \right)^3 \right) - \sigma B_0^2 w - \frac{\mu w}{K_p^*} \tag{15}$$

Equation (15) represents the flow due to pressure gradient. After leaving the die, there is only drag of the wire. So the pressure gradient in the axial direction is taken to be zero. Hence, equation (15) becomes

$$\frac{2(\beta_2+\beta_3)}{r}.\frac{d}{dr}\left(r\left(\frac{dw}{dr}\right)^3\right)+\frac{1}{r}\frac{d}{dr}\left(\mu r\frac{dw}{dr}\right)-\sigma B_0^2 w-\frac{\mu w}{K_p^*}=0 \tag{16}$$

and the energy equation (8) becomes

$$k\left(\frac{d^2}{dr^2}+\frac{1}{r}\frac{d}{dr}\right)\theta+\mu\left(\frac{dw}{dr}\right)^2+2(\beta_2+\beta_3)\left(\frac{dw}{dr}\right)^4+Q_0(\theta-\theta_w)+\sigma B_0^2 w^2=0 \tag{17}$$

2.1 Constant Viscosity

Introducing the dimensionless parameters

$$\left.\begin{aligned} &r^*=\frac{r}{R_w},\quad w^*=\frac{w}{U_w},\quad \theta^*=\frac{\theta-\theta_w}{\theta_d-\theta_w},\ \beta_0=\beta_2+\beta_3\\ &\frac{R_d}{R_w}=\delta>1, M^2=\frac{\sigma B_0^2 R_w^2}{\mu}, K_p=\frac{R_w^2}{U_w K_p^*}, Q=\frac{Q_0 R_w^2}{k}\end{aligned}\right\} \tag{18}$$

The system of equations (2), (16) and (17) after dropping the asterisks, become

$$r\frac{d^2w}{dr^2}+\frac{dw}{dr}+2\beta_0\left[3r\frac{d^2w}{dr^2}\left(\frac{dw}{dr}\right)^2+\left(\frac{dw}{dr}\right)^3\right]-\left(M^2+K_p\right)wr=0 \tag{19}$$

$$w(1)=1 \ \text{and} \ \ w(\delta)=0 \tag{20}$$

$$\frac{d^2\theta}{dr^2}+\frac{1}{r}\frac{d\theta}{dr}+B_r\left(\frac{dw}{dr}\right)^2+2B_r\beta_0\left(\frac{dw}{dr}\right)^4+Q\theta+B_r M^2 w^2=0 \tag{21}$$

$$\theta(1)=0 \ \text{and} \ \ \theta(\delta)=1 \tag{22}$$

where the Brinkman number (B_r) and non-Newtonian parameter (β_0) are given by

$$B_r=\frac{\mu U_w^2}{k(\theta_d-\theta_w)} \ \text{and} \ \ \beta_0^*=\frac{\beta_0}{\mu\left(\frac{R_w^2}{U_w^2}\right)} \quad \text{respectively.}$$

(i) Numerical Solution

The Runge-Kutta method has been used to solve equations (19) and (21) with boundary conditions (20) and (22). These equations are reduced to system of first order differential equations since for the equations of higher order the value at $r=\delta$ (thickness of boundary layer) is not available. Therefore, the shooting method is used to solve the boundary value problem. The physical and computation domains are finite. For computational purpose we have taken $\delta=2$.

2.2 Variable Viscosity/ Temperature dependent Viscosity

2.2.1 Reynolds Model

In this case, Reynolds model is used to account for the temperature dependent viscosity.
For Reynolds model, the dimensionless viscosity is

$$\mu = exp\left(-\beta_0 m\theta\right) \approx 1-\beta_0 m\theta \tag{23}$$

which can be used for variation of viscosity with temperature where *m* is the viscosity parameter.

Non-dimensional momentum and energy equations with boundary conditions omitting asterisks are

$$(1-\beta_0 m\theta)\left(r\frac{d^2w}{dr^2}+\frac{dw}{dr}-K_p wr\right)+2\beta_0\left[3r\frac{d^2w}{dr^2}\left(\frac{dw}{dr}\right)^2+\left(\frac{dw}{dr}\right)^3\right]-\beta_0 m\frac{d\theta}{dr}\frac{dw}{dr}-M^2wr=0 \tag{24}$$

$$w(1)=1 \text{ and } w(2)=0 \tag{25}$$

$$\frac{d^2\theta}{dr^2}+\frac{1}{r}\frac{d\theta}{dr}+(1-\beta_0 m\theta)B_r\left(\frac{dw}{dr}\right)^2+2B_r\beta_0\left(\frac{dw}{dr}\right)^4+Q\theta+B_r M^2w^2=0 \tag{26}$$

$$\theta(1)=0 \text{ and } \theta(2)=1 \tag{27}$$

The non-dimensional parameters are

$$\left.\begin{aligned} r^*=\frac{r}{R_w}, w^*=\frac{w}{U_w}, \theta^*=\frac{\theta-\theta_w}{\theta_d-\theta_w}, \beta_0=\beta_2+\beta_3, \frac{R_d}{R_w}=\delta>1 \\ B_r=\frac{\mu_0 U_w^2}{k(\theta_d-\theta_w)}, \mu^*=\frac{\mu}{\mu_0}, \beta_0^*=\frac{\beta_0}{\left(\frac{R_w\mu_0}{U_\infty^2}\right)}, M^2=\frac{\sigma B_0^2 R_w^2}{\mu_0}, K_p=\frac{R_w^2}{U_w K_p^*} \end{aligned}\right\} \tag{28}$$

where μ_0 is a reference viscosity.

Numerical Solution

Equations (24) and (26) with boundary condition (25) and (27) are solved numerically applying Runge-Kutta method as mentioned in constant viscosity case.

2.2.2 Vogel's Model

In this case, the temperature dependent viscosity is taken as

$$\mu=\mu_0 \exp\left(\frac{D}{B'+\theta}-\theta_w\right) \tag{29}$$

Using expansion, we have

$$\mu=\Omega_1\left(1-\frac{D}{B'^2}\theta\right) \tag{30}$$

where $\Omega_1=\mu_0\exp\left(\frac{D}{B'}-\theta_w\right)$ and D, B' are viscosity parameters associated with Vogel's model.

So the non-dimensional momentum and energy equations with boundary conditions omitting asterisk are

$$\Omega_1\left(1-\frac{D}{B'^2}\theta\right)\left(r\frac{d^2w}{dr^2}+\frac{dw}{dr}-K_p wr\right)+2\beta_0\left[3r\frac{d^2w}{dr^2}\left(\frac{dw}{dr}\right)^2+\left(\frac{dw}{dr}\right)^3\right]-\left(\frac{\Omega_1 D}{B'^2}\right)\frac{d\theta}{dr}\frac{dw}{dr}-M^2wr=0 \tag{31}$$

$$w(1)=1 \text{ and } w(2)=0 \tag{32}$$

$$\frac{d^2\theta}{dr^2}+\frac{1}{r}\frac{d\theta}{dr}+\Omega_1\left(1-\frac{D}{B'^2}\theta\right)B_r\left(\frac{dw}{dr}\right)^2+2B_r\beta_0\left(\frac{dw}{dr}\right)^4+Q\theta+B_rM^2w^2=0 \quad (33)$$

$$\theta(1)=0 \text{ and } \theta(2)=1 \quad (34)$$

Numerical Solution

The numerical solutions of equations (31) and (33) with the boundary condition (32) and (34) can be obtained with $D=\beta_0 b$. During the numerical computation by Runge-Kutta method we have assigned different values to viscosity parameter (Ω_1) and the values of B' and *b* are assigned as B' = 0.2 and *b* = 0.5. The numerical solutions of velocity and temperature distributions are presented through graphs.

3. Results and Discussion

The following discussion presents the comparative case study of constant viscosity and variable viscosity comprising of Reynolds model and Vogel's model related to wire coating process using melt polymer satisfying third grade fluid model in a pressure type die. The Runge-Kutta method with shooting technique has been applied to solve the governing equations.

The effects of various pertinent parameters such as non-Newtonian parameter β_0, permeability parameter K_p, Reynolds model viscosity parameter *m*, Vogel's model viscosity parameter Ω_1, heat generation/absorption parameter *Q* and Brinkman number B_r, are discussed.

The flow and heat transfer phenomena occurring inside the wire coating dies determine the quality of the coated wire produced.

3.1 Case of Constant Viscosity

Fig.3 delineates the effects of permeability parameter (K_p) and non-Newtonian parameter (β_0) on the velocity field. It is noticed that the permeability parameter (K_p) decreases the velocity field in case of both Newtonian and non-Newtonian fluids in absence of heat generation/absorption. It is also further noticed that an increase in non-Newtonian parameter, keeping the permeability parameter fixed, leads to increase the velocity at all points of the flow domain in absence of heat generation/absorption. Hence the permeability parameter contributes to slow down the velocity where as non-Newtonian parameter characterizing the melt polymer (third grade fluid) accelerates it.

Fig. 4 exhibits the temperature distribution in case of third grade fluid when non-Newtonian parameter, $\beta_0=0.1$ in presence of Joule heating. Since the curves for $K_p=0$ and $K_p=2$ coincide, the effect of permeability parameter is not significant irrespective of low/high values of Brinkman number (B_r). However, an increase in B_r leads to increase the temperature at all points significantly in the absence of heat generation/absorption. Hence, it is remarked that in the process of wire coating, the Brinkman number, the relative measure of viscous heating with heat conducted, enhances the temperature significantly at all points whereas porous matrix has no remarkable contribution.

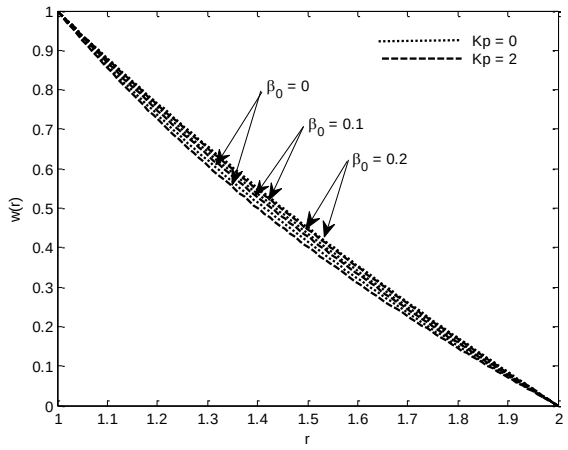

Fig. 3 Velocity distributions (Constant viscosity) showing the effect of β_0 and K_p for $B_r = 5, M = 0.5, R = 2, Q = 0$.

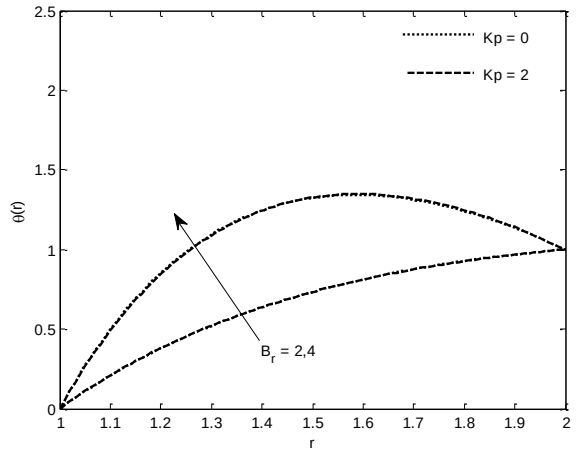

Fig. 4 Temperature distributions (constant viscosity) showing the effect of B_r and K_p for $\beta_0 = 0.1, M = 0.2, R = 2, Q = 0$.

3.2 Case of Variable Viscosity

3.2.1 Reynolds Model

Fig. 5 shows the velocity distribution when the Brinkman number, viscosity parameter, magnetic parameter and heat generation/absorption parameter are set to fixed values. It is observed that the non-Newtonian parameter β_0 is to increase the velocity both in the presence or absence of porous matrix but the reverse effect is observed in case of porous matrix. Thus, it is to note that non-Newtonian property of the fluid is favourable for enhancing the velocity in conjunction with temperature dependent variable viscosity in absence of heat generation/absorption.

Fig.6 delineates the velocity variation for different values of viscosity parameter and permeability parameter. It is seen that viscosity parameter enhances the velocity at all points in the presence/absence of porous matrix without heat generation/absorption.

From Fig. 7 it is noticed that increase in magnetic field strength contributes to slow down the velocity in entire flow domain in the absence of heat generation/absorption.

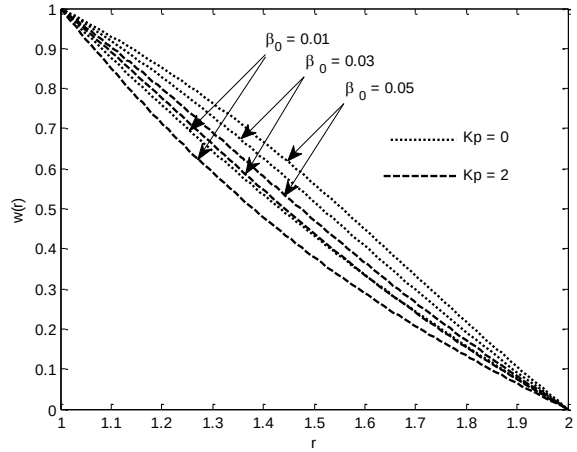

Fig. 5 Velocity distributions (Reynolds model) showing the effect of K_p and β_0 for $B_r = 10$, $m = 10, M = 1, R = 2, Q = 0$.

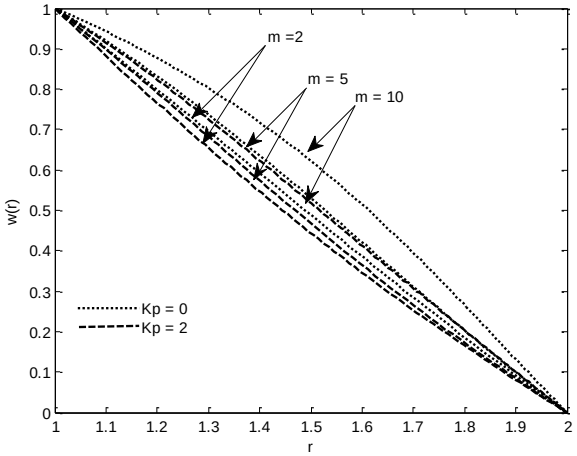

Fig. 6 Velocity distributions (Reynolds model) showing the effect of *m* and K_p for $B_r = 10, R = 2$, $M = 0.5,\ \beta_0 = 0.1, Q = 0$.

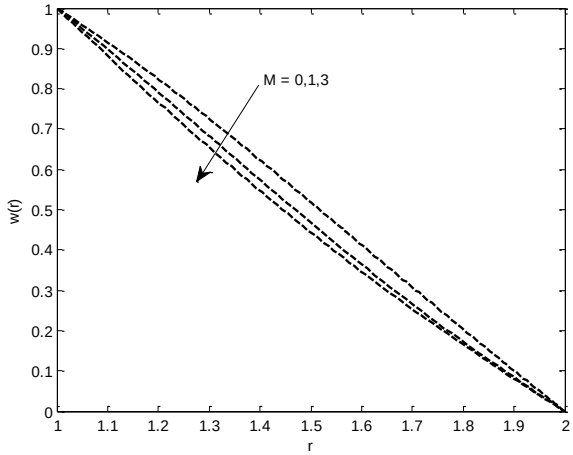

Fig. 7 Velocity distributions (Reynolds model) showing the effect of *M* for $B_r = 10, R = 2, m = 5, K_p = 2,\ \beta_0 = 0.1, Q = 0$.

From Fig. 8 it is observed that for a fixed value of viscosity parameter, magnetic parameter and heat generation/absorption parameter, the temperature increases with an increase in Brinkman number in the presence as well as absence of the porous matrix associated with Joule heating. It is also observed that an increase in porous matrix leads to higher temperature within the layers r < 1.6, thereafter, the temperature decreases. This is because the resistive force offered by porous matrix is dominated by the boundary surface effects.

Fig. 9 illustrates that an increase in magnetic field leads to higher temperature within the layers r < 1.6 thereafter, the temperature decreases. This scenario is due to the fact that the boundary surface effect overrides the effects of magnetic field.

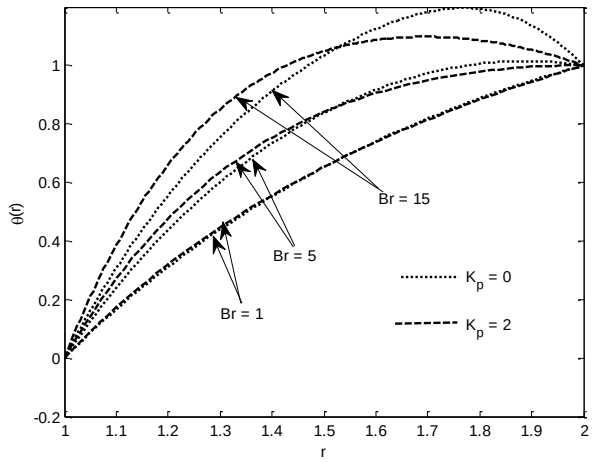

Fig. 8 Temperature distributions (Reynolds Model) showing the effect of K_p and B_r for $\beta_0 = 0.1$, $m = 10, M = 0.5, R = 2, Q = 0$.

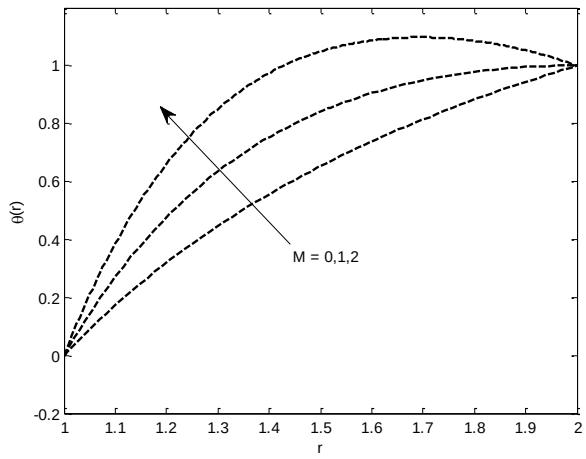

Fig. 9 Temperature distributions (Reynolds Model) showing the effect of *M* for $\beta_0 = 0.1$, $m = 10, K_p = 2, R = 2, B_r = 4, Q = 0$.

Fig. 10 displays the effect of heat generation/absorption parameter on temperature distribution. It shows that heat generation in thermal boundary layer causes the temperature to rise whereas the heat absorption in thermal boundary layer results in decreasing temperature.

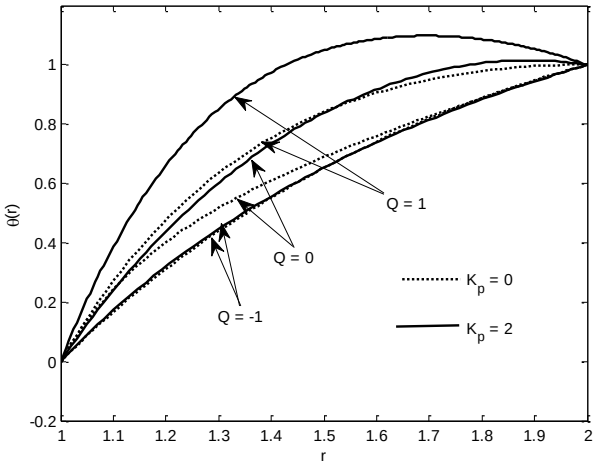

Fig. 10 Temperature distributions (Reynolds Model) showing the effect of *Q* and K_p for $\beta_0 = 0.1$, $m = 10, M = 0.5, R = 2, B_r = 2$.

3.2.2 Vogel's Model

Fig. 11 displays two layer velocity distributions, one for conducting fluid and the other one for non-conducting fluid, indicating decelerating effects offered by the resistive force of porous matrix in the absence of heat generation/absorption. Another interesting aspect is the occurrence of point of inflexion vis-à-vis point of intersection in the middle of the annular region which recedes slightly towards *r* = 1.0. This indicates that transition sets in little ahead in presence porous matrix. It is also evident that increase in viscosity parameter (Ω_1) accelerates the velocity in the region 1.0 < r < 1.6 for presence/absence of porous matrix. On the other hand, reverse effect is observed after words. This shows that near the surface of the wire, velocity gets accelerated irrespective of porous matrix. It is worth mentioning here that in case of constant viscosity as well as variable viscosity (Reynolds model), the porous matrix decreases the velocity throughout the flow field. Again comparing the effect of variable viscosity in Reynolds model and Vogel's model it is found that viscosity parameter accelerates the velocity throughout the case of Reynolds model where as it is confined to 1 < r <1.6 in case of Vogel's model irrespective of the effect of porosity.

The effect of magnetic field is similar to the effect of porosity as shown in Fig. 12. However, a striking feature is observed that the variation of viscosity parameter is prominent irrespective magnetic field. Also it is observed that the variation of viscosity is significant in presence/absence of magnetic field than that in presence/absence of porous matrix. This indicates that the resistance offered by the Lorentz force due to the presence of magnetic field overrides the resistance offered by the porous matrix. Another interesting feature is that $\Omega \neq 0$ imposes a transition in motion within the same layer (r < 1.6) of melt polymer in absence/presence of magnetic field.

Fig. 13 shows that an increase in Brinkman number increases the velocity in the absence of porous matrix, whereas in the presence of porous matrix, the effect of B_r is not significant when $1 < r < 1.25$ but thereafter, the decrease in velocity occurs with an increase in B_r, i.e. with the rise of viscous heating. One aspect is very much clear from Fig. 15 that viscous heating ($B_r \neq 0$) with or without porous matrix has a distinct role to play in reducing the velocity as well as developing a transition state on fluid property in the absence of heat generation/absorption.

Fig.14 shows the effects of non-Newtonian parameter β_0. It is seen that an increase in non-Newtonian parameter increases the velocity in the region 1 < r < 1.45 both in the presence or

absence of porous matrix, after words, it decreases. Thus, it is concluded that non-Newtonian property of fluid enhances the velocity of the coating material near the surface of the wire then it decreases but an increase in permeability parameter (K_p) with higher non-Newtonian parameter reduces the velocity throughout the annular region. Further it is remarked that for higher values of non-Newtonian and permeability parameters the velocity is reduced significantly almost at all points.

It is remarkable to note from Fig. 15 that increase of variable viscosity and viscous heating cause thermo-transitions to take place in the absence/presence of porous matrix in association with Joule heating. The effect of porous matrix with viscous heating or variable viscosity enhances the temperature just immediate from the surface of the wire, but thereafter the reverse effect is observed. The same thermal characteristics are visualized in case of magnetic field, however, with moderately greater magnitude as shown in Fig. 16.

It is important to note that the flow instability is well marked from Figs 11-14 in case of Vogel's model and slightly from Fig 8 in case of Reynolds model. This observation coincides with Nhan-Phan-Thien [26]. As pointed, the non-linearity in the constitutive equations makes viscoelastic flows full of instabilities such as in the flows of extrusion dies.

Figs. 17 and 18 delineate the temperature distribution showing the effects of Brinkman number with permeable parameter as well as magnetic parameter in the absence of heat generation/absorption. The point of thermo-transition occurs in the middle of the annular zone. The effects of porous matrix, magnetic parameter and Brinkman number are to increase the temperature in the first half in all the cases, the reverse effect is observed. Thus it is concluded that viscous heating (B_r) and non-Newtonian property of melt polymer are favourable in escalating the fluid temperature in the layers near the surface of the wire and it is counterproductive near the inner surface of the die.

Fig. 19 portrays the effect of heat generation/absorption parameter on temperature distribution by setting the fixed values of β_0, K_p, M, B_r and Ω_1. It shows that heat generation in thermal boundary layer causes the temperature to rise leading to increase in heat transfer rate and hence enhances the thermal boundary layer thickness whereas the opposite effect is observed in case of heat absorption.

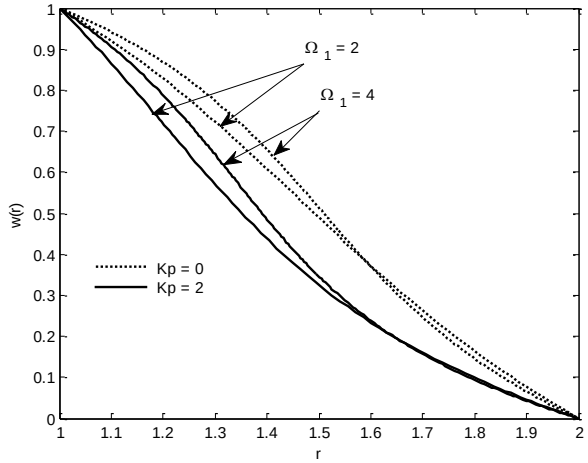

Fig. 11 Velocity distributions (Vogel's model) showing the effect of K_p and Ω_1 for

$B_r = 15, R = 2, M = 2,\ \beta_0 = 0.1, Q = 0.$

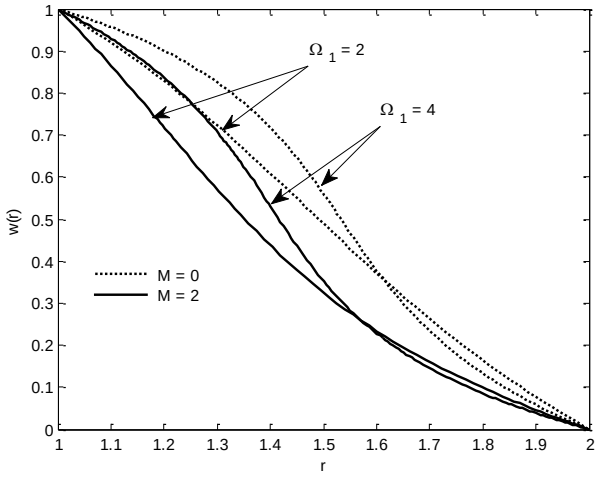

Fig. 12 Velocity distributions (Vogel's model) showing the effect of *M* and Ω_1 for $B_r = 15, R = 2, K_p = 2,\ \beta_0 = 0.1, Q = 0$.

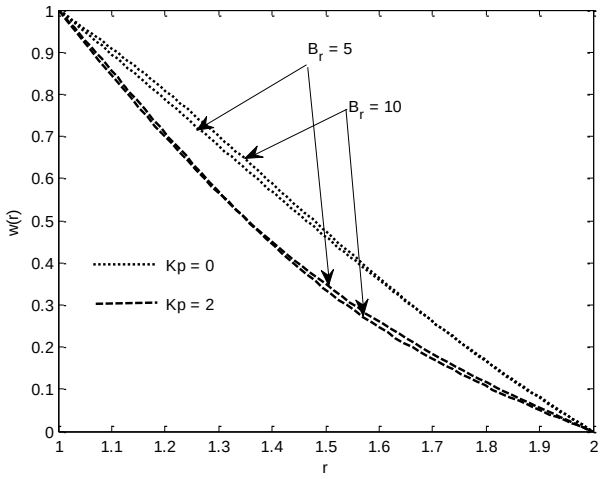

Fig. 13 Velocity distributions (Vogel's model) showing the effect of B_r and K_p for $\beta_0 = 0.05, M = 2, R = 2,\ \Omega_1 = 2, Q = 0$.

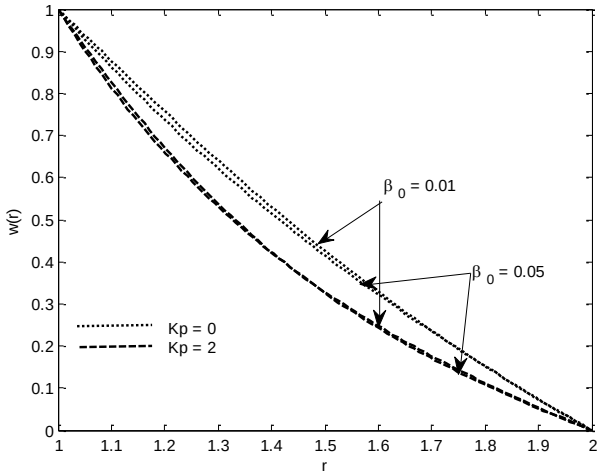

Fig. 14 Velocity distributions (Vogel's model) showing the effect of β_0 and K_p for $M = 2, \Omega_1 = 2, R = 2,\ B_r = 15, Q = 0$.

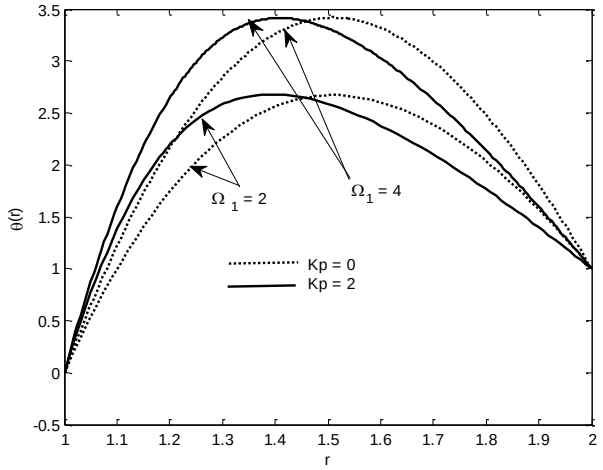

Fig.15 Temperature distributions (Vogel's model) showing the effect of Ω_1 and K_p for $\beta_0 = 0.05, M = 1, R = 2,\ B_r = 15, Q = 0$.

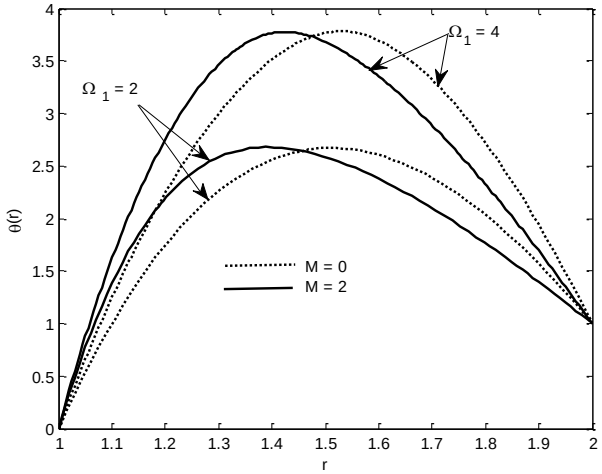

Fig.16 Temperature distributions (Vogel's model) showing the effect of Ω_1 and *M* for $\beta_0 = 0.05, K_p = 2, R = 2,\ B_r = 15, Q = 0$.

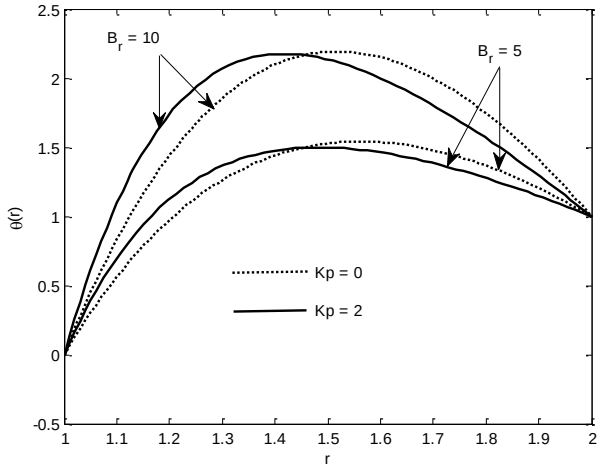

Fig. 17 Temperature distributions (Vogel's model) showing the effect of B_r and K_p for $\beta_0 = 0.05, M = 1, R = 2,\ \Omega_1 = 2, Q = 0$.

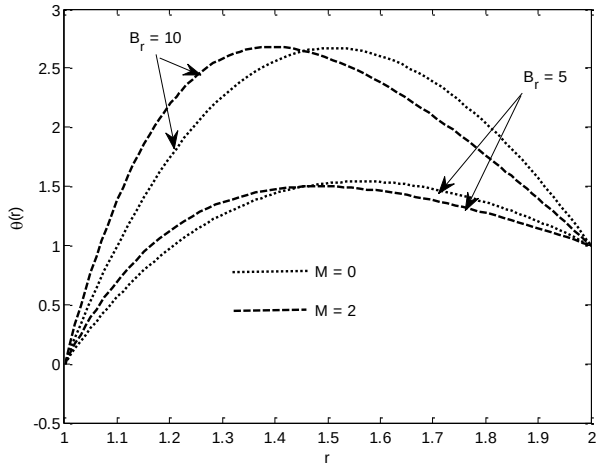

Fig. 18 Temperature distributions (Vogel's model) showing the effect of B_r and *M* for $\beta_0 = 0.05, K_p = 2, R = 2, \ \Omega_1 = 2, Q = 0$.

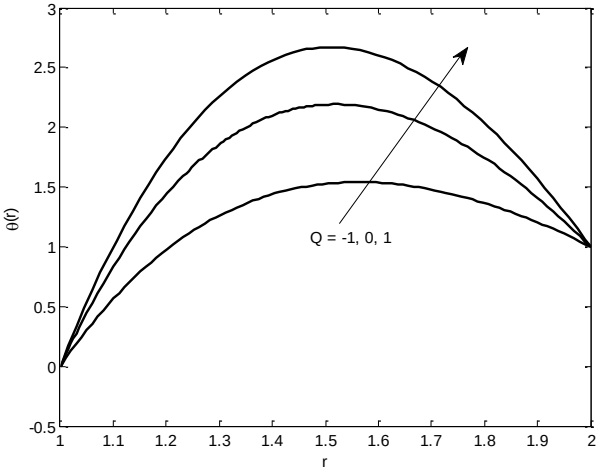

Fig. 19 Temperature distributions (Vogel's model) showing the effect of *Q* for $\beta_0 = 0.05, K_p = 2, M = 1, B_r = 15, \ \Omega_1 = 2, R = 2$.

4. Conclusion

4.1 Case of Constant Viscosity

1. Porous matrix contributes to slow down the velocity whereas non-Newtonian parameter characterizing the melt polymer (third grade fluid) accelerates it. As the velocity of coating fluid is an important design requirement, porous matrix and non-Newtonian characteristics of fluid may be used as controlling devices for the required quality of the wire-coating.
2. In the process of wire coating, the Brinkman number, which is the relative measure of viscous heating with heat conducted, enhances the temperature significantly at all points where as porous matrix has no remarkable contribution.

4.2 Case of Variable Viscosity

Reynolds Model

3. Non-Newtonian property of the fluid is favourable for enhancing the velocity in conjunction with temperature dependent variable viscosity.

4. On comparison with constant viscosity case, it is remarked that effects of non-Newtonian property of the fluid and porosity remain unaltered but the deceleration of fluid velocity is significant in case of temperature dependent variable viscosity.
5. Heat generation in thermal boundary layer leads to temperature rise whereas the heat absorption in thermal boundary layer results in decreasing temperature.

Vogel's Model

6. Vogel's model contribute two layer velocity distribution, one for conducting fluid and the other one for non-conducting fluid, indicating decelerating effects due to resistive force offered by magnetic field as well as porous matrix. Another interesting aspect is the occurrence of point of inflexion vis-à-vis point of intersection in the middle of the annular region.
7. It is worth mentioning here that in case of constant viscosity as well as variable viscosity (Reynolds model), the magnetic field as well as porous matrix decrease the velocity throughout the flow field. Again comparing the effect of variable viscosity (Reynolds model) with Vogel's it is found that viscosity parameter accelerates the velocity throughout the case of Reynolds model whereas it is confined to $1 < r < 1.6$ (Vogel's model) irrespective of the effect of porosity.
8. The effect of variable viscosity is decisive and significant in enhancing the temperature throughout the flow region under investigation. While comparing with the Reynolds model it is revealed that the fluid gets heated with porous matrix and viscosity parameter in both the cases. Both the models have same effect in response to porous matrix by increasing the temperature nearer to the wire-surface and having a transition in the middle of the annular region.
9. The viscoelastic flows are full of instabilities such as in the flows of extrusion dies as claimed by Nhan-Phan-Thien is also observed in the present study.
10. Heat generation in thermal boundary layer causes the temperature to rise leading to increase in heat transfer rate and hence enhances the thermal boundary layer thickness whereas the opposite effect is observed in case of heat absorption.

References

[1] C. D. Han, D. Rao, The rheology of wire coating extrusion, Polym. Eng. Sci., 18 (13) (1978) 1019-1029.

[2] B. Caswell, R. J. Tanner, Wire coating die using finite element methods, Polym. Eng. Sci., 18(5) (1978) 417-421.

[3] C. L. Tucker, Computer Modeling for Polymer Processing, Hanser, Munich, (1989) 311-317.

[4] M. K. Nayak, Wire coating analysis, 2nd ed., India Tech, New Delhi, (2015).

[5] S. Akter, M. S. J. Hashmi, Wire drawing and coating using a combined geometry hydrodynamic unit, J. Material Proc. Tech., 178 (2006) 98-110.

[6] Z. Tadmor, C.G. Gogos, Principle of Polymer Processing, John Wiley and Sons, New York, (1979).

[7] A. Fata, N. Moallemi, S. Latifzadeh, I. Shafieenejad, S. F. Hashemi, Wire coating analysis using magneto-hydrodynamic flow of a third grade fluid, Int. Review of Mechanical Engineering, 5(3) (2011) 533.

[8] A.M. Siddiqui, T. Haroon and H. Khan, Wire coating extrusion in a pressure type die in flow of a third grade fluid, Int. J. of Non-Linear Sci. Numeric. Simul., 10(2) (2009) 247-257.

[9] T. Hayat, A. Shafiq , A. Alsaedi, MHD axisymmetric flow of third grade fluid by a stretching cylinder, Alexandria Engineering Journal, 54 (2) (2015) 205–212.

[10] H. Shuaib, T. Gul , M. A. Khan, S. Islam, S. Nasir, Z. Shah, M. Ayaz, F. Ghani, Heat Transfer and Unsteady MHD Flow of Third Grade Fluid Past on Vertical Oscillating Belt, J. Appl. Environ. Biol. Sci., 5(5) (2015) 25-34.

[11] T. Chinyoka, O. D. Makinde, Unsteady hydromagnetic flow of a reactive variable viscosity third-grade fluid in a channel with convective cooling, Int. J. Numer. Methods in Fluids 69(2) (2012) 353–365.

[12] M. Kasajima, K. Ito, Post-treatment of Polymer extrudate in wire coating, Appl. Polym. Symp., 20 (1973) 221-235.

[13] R. Wagner, E. Mitsoulis, Effect of die design on the analysis of wire coating. Adv. Polym. Tech., 5 (1985) 305-325.

[14] E. B. Bagley, S. H. Storey, *Wire Wire Prod.*. 38 (1963) 1104.

[15] Z. Tadmor, R.B. Bird, Rheological analysis of stabilizing forces in wire-coating dies, Polym. Eng. Sci., 14 (1974) 124.

[16] D. B. Ingham, I Pop, Transport phenomena in Porous Media, Elsevier Sc. Ltd., U. K., (1998).

[17] K. Vafai, Handbook of Porous Media, 2nd ed., Taylor and Francis, New York, (2005).

[18] I. A. Nield, A. Bejan, Convection in Porous Media, 4th ed., Springer, New York, (2012).

[19] A. Bejan, Convection Heat Transfer, 4th ed., Wiley, New York, (2013).

[20] M. K. Nayak, Flow through porous media, 1st ed., India Tech, New Delhi, (2014).

[21] M. K. Nayak, G. C. Dash, L. P. Singh, Effect of chemical reaction on MHD flow of a visco-elastic fluid through porous medium, J. Appl. Anal. Comput., 4(4) (2014) 367-381.

[22] G. C. Dash, S. S. Dash, S. K. Sahoo, MHD flow and heat transfer of a viscous electrically conducting fluid past a stretching sheet through a porous medium, AMSE Journals, Series: Modelling B, 75(4) (2006) 41-56.

[23] M. K. Nayak, G.C. Dash, L.P. Singh**,** Flow and mass transfer analysis of a micropolar fluid in a vertical channel with heat source and chemical reaction, AMSE Journals, Series: Modelling B, 84 (1) (2015) 69-91.

[24] M. K. Nayak, G. C. Dash, L. P. Singh, Unsteady radiative MHD free convective flow and mass transfer of a viscoelastic fluid past an inclined porous plate, Arab. J. Sci. Eng., DOI 10.1007/s13369-015-1805-8 (2015).

[25] M. K. Nayak, G. C. Dash, L. P. Singh, Steady MHD flow and heat transfer of a third grade fluid in wire coating analysis with temperature dependent viscosity, Int. J. Heat Mass Transfer, 79 (2014) 1087–1095.

[26] Nhan-Phan-Thien, Understanding visco-elasticity, 2nd ed., Springer, p-38.